Synthesis and Characterization of a Novel Charring Agent and Its Application in Intumescent Flame Retardant Polypropylene System

Jianqian Huang,[1] Yeqin Zhang,[2] Qi Yang,[1,3] Xia Liao,[1,3] Guangxian Li[1,3]

[1]*College of Polymer Science & Engineering, Sichuan University, Chengdu 610065, People's Republic of China*
[2]*China Bluestar Chengrand Chemical Co., Ltd., Chengdu 610065, People's Republic of China*
[3]*State Key Laboratory of Polymer Materials Engineering, Sichuan University, Chengdu 610065, People's Republic of China*

Received 19 November 2010; accepted 25 March 2011
DOI 10.1002/app.34578
Published online 19 August 2011 in Wiley Online Library (wileyonlinelibrary.com).

ABSTRACT: A novel halogen-free charring agent bi(4-methoxy-1-phospha-2, 6, 7-trioxabicyclo [2.2.2]-octane-1-sulfide) phenylphosphate (BSPPO) was synthesized from phenylphosphonic dichloride (PPDC), and 4-hydroxymethyl-1-phospha-2, 6, 7-trioxabicyclo[2.2.2]-octane-1-sulfide (SPEPA) which was synthesized from pentaerythritol and thiophosphoryl chloride in this article. The structure of BSPPO and SPEPA was characterized by Fourier transform infrared (FTIR), ^{1}H-NMR, ^{13}C-NMR, and ^{31}P-NMR. Combined with ammonium polyphosphate (APP) and melamine pyrophosphate (MPP), the flame retardance and dripping resistance of BSPPO added in polypropylene (PP) were investigated. The fire performance of the flame retardant PP system was investigated by limiting oxygen index (LOI), vertical burning test (UL-94), and cone calorimeter. The thermal stabilities of the composites were studied by thermogravimetric analysis (TGA). The flame retardance mechanism was investigated by FTIR and scanning electronic micrograph (SEM). The mechanical properties and water solubility were also investigated. The residue of BSPPO is 40.6% at 600°C, which indicates BSPPO has excellent charring ability. The char residue of the polypropylene intumescent flame retardant (PP-IFR) system is 22% at 600°C, which suggests that the flame retardation synergy of APP, BSPPO, and MPP is good. With the optimum formulation, the LOI of the IFR-PP system is 32.0, and the UL-94 is V-0 rating. The heat release rate (HRR), total heat release (THR), smoke production rate (SPR), total smoke production (TSP), and mass loss rate (MLR) of IFR-PP with the optimum formulation decrease significantly comparing to pure PP from cone calorimeter analysis. The FTIR and SEM results indicate that the char properties and the char yield have direct effect on the flame retardance and antidripping behaviors. © 2011 Wiley Periodicals, Inc. J Appl Polym Sci 123: 1636–1644, 2012

Key words: charring agent; intumescence; flame retardance; polypropylene; phenylphosphonic dichloride

INTRODUCTION

Polypropylene (PP) is used worldwide for many applications. However, PP is a highly combustible material that burns with flammable dripping. In addition, it releases smoke and poisonous gases during the fire because of the aliphatic hydrocarbon structure. So flame retardance becomes an important requirement for PP. Traditionally, halogen-containing compounds with antimony trioxide as a synergistic agent are the main flame retardants of PP. However, some of them are limited in use because of the evolution of toxic gases and corrosive smoke during combustion and dioxins problem and other environmental problems.[1–3] Now halogen-free compounds are regarded as promising flame retardants because of their environmentally friendly properties. Among them metal hydroxides such as $Mg(OH)_2$ and $Al(OH)_3$ are commonly used, but highly loading (more than 60 wt %) of the metal hydroxides is required to obtain an adequate flame retardant property at the expense of the rheological and mechanical properties of the flame retardant materials.[4–6] In recent years, intumescent flame retardants (IFR) have attracted increasing attention in the flame retardation of materials because they produce low smoke and toxicity with no corrosive gas generation. The IFR system is usually composed of three components: an acid source, a carbonization agent, and a blowing agent.[7–16] A typical and widely adopted IFR system is an ammonium polyphosphate (acid source)/pentaerythritol (carbonization agent)/melamine (blowing agent; APP/PER/MA) mixture.[17–19] However, the hydrophilic properties of PER because of four hydroxyl groups in the structure make this

Correspondence to: Q. Yang (yangqi@scu.edu.cn).
Contract grant sponsor: State Key Laboratory Special Fund, Program for New Century Excellent Talents in University; contract grant number: NCET-10-0576.
Contract grant sponsor: National Natural Science Foundation of China; contract grant number: 50773042.

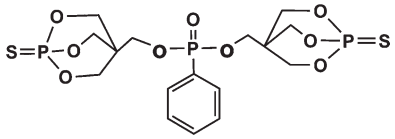

Scheme 1 Chemical structure of BSPPO.

IFR system moisture sensitive, which will decrease flame retardancy of PP because of the exudation of the additive. Many researchers try to avoid problems of exudation and water solubility of PER.[20–22] Ratz and Sweeting[23] synthesized the derivative of PER, namely, 4-hydroxymethyl-1-phospha-2, 6,7-trioxabicyclo[2.2.2]-octane-1-sulfide (SPEPA). However, it has still a hydroxyl group in its structure, and the content of carbon is only 30.62%.

To avoid the defect and to increase the char residue, a novel halogen-free phosphorus-containing caged bicyclic carbonization agent [bi(4-methoxy-1-phospha-2, 6, 7-trioxabicyclo [2.2.2]-octane-1-sulfide) phenylphosphate (BSPPO), Scheme 1], which is hydrophobic in nature and shows high thermal stability because of the symmetrical structure and the incorporation of carbon abounding benzene group, was synthesized by a nucleophilic substitution reaction under low temperature successfully. The structure of BSPPO was characterized by Fourier transform infrared (FTIR), ^{1}H-NMR, ^{13}C-NMR, ^{31}P-NMR. The thermal properties and flammability of intumescent flame retardant polypropylene (IFR-PP) system using BSPPO as carbonization agent combining with APP as well as melamine pyrophosphate (MPP) were investigated. The mechanical properties and water solubility were also investigated.

EXPERIMENTAL

Materials

PP (T30S) with a MFI of 3.0 g (10 min)$^{-1}$ was provided by China Petroleum and Chemical Corp. Maoming Branch (Maoming, China). Its melting temperature (T_m) was 150°C tested through a differential scanning calorimetry (DSC204, NETZSCH, Germany) with scanning rate of 10°C min^{-1}.

Thiophosphoryl chloride ($PSCl_3$), PER, and phenylphosphonic dichloride (PPDC) supplied by Changzheng Chemical Reagent Corp. (Chengdu, China). APP was provided by Changfeng Chemical Corp. (Shifang, China). MPP was provided by Fine Chemical Engineering Research and Design Institute of Sichuan.

Preparation of 4-hydroxymethyl-1-phospha-2,6,7-trioxabicyclo[2.2.2]-octane-1-sulfide

A mixture of 62.6 g (0.46 mol) PER and 77.9 g (0.46 mol) thiophosphoryl chloride was heated at 145°C in a 250-mL round-bottomed flask equipped with reflux, protected from atmospheric moisture and equipped with magnetic stirrer. Evolution of hydrogen chloride ceased after 10 h. The resulting cake was extracted with 250 mL boiling water and cooled to room temperature. During the extracting some material remained undissolved and collected as heavy oil at the bottom of the flask. The aqueous solvent was separated from this oil by decantation through a folded filter. The product was crystallized from water and afforded white crystals (62 g, yield 68.7%, m.p. 158–160°C).

Preparation of bi(4-methoxy-1-phospha-2, 6, 7-trioxabicyclo [2.2.2]-octane-1-sulfide) phenylphosphate

A 250-mL three-necked round bottom flask was equipped with a magnetic stirrer, a reflux condenser, and a constant pressure funnel. The flask was charged with 19.6 g (0.1 mol) SPEPA, 10.1 g (0.1 mol) triethylamine, and 80 mL acetonitrile. Thereafter, the mixture was stirred and heated to reflux. Then 9.8 g (0.05 mol) PPDC was added within 0.5 h, and the reaction was kept about 8 h at the same temperature. Successively, the reaction mixture was cooled to room temperature, then poured the mixture into distilled water and filtered. The solid was washed with ethanol and dried at 100°C under vacuum to constant weight (product yield: 86.37%). Melt point is over 300°C (decomposition).

Preparation of test samples

All samples were prepared in a parallel corotating twin-screw extruder with a length/diameter ratio of 32, and a screw diameter of 25 mm (TSSJ-25/32, provided by the Research Institute of Plastic Machine of ChenGuang, Chengdu, China). The composites were extruded at 190°C with 90 rpm. The samples were hot-pressed under 10 MPa for 5 min at 190°C into sheets of suitable thickness and size according to ASTM D2863-97, ASTM D3801, and ISO 5660.

Characterization

FTIR spectra were recorded on a Nicolet FTIR 170SX infrared spectrophotometer using KBr pellets. ^{1}H-

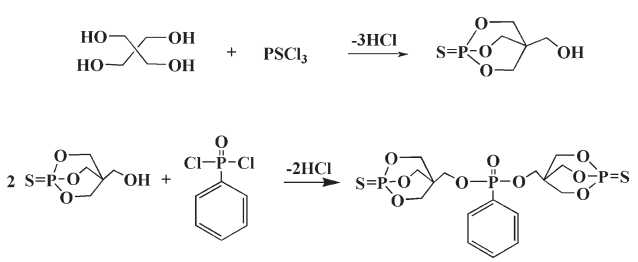

Scheme 2 Synthesis route of BSPPO.

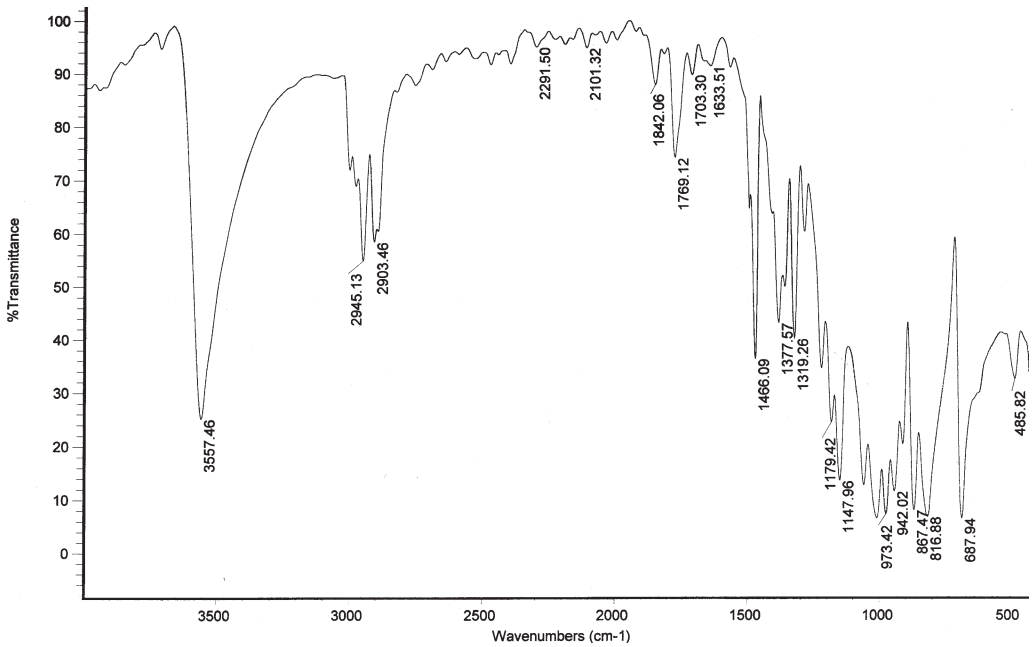

Figure 1 FTIR spectrum of SPEPA.

NMR, ^{13}C-NMR, and ^{31}P-NMR were carried out on a Bruker AV II-400 MHz, using DMSO-d_6 as solvent and TMS as an internal standard.

Limiting oxygen index (LOI) values were measured on a HC-2 oxygen index meter (Jiangning Analysis Instrument Company, China) with sheet dimensions of 130 × 6.5 × 3 mm^3, according to ASTM D2863-97. The vertical burning tests (UL-94) were conducted on a CFZ-2-type instrument (Jiangning Analysis Instrument Company, China) with sheet dimensions of 130 × 13 × 3 mm^3, according to ASTM D3801.

Heat release rate (HRR), peak of HRR (PHRR), total heat release (THR), smoke production rate (SPR), total smoke production (TSP), and mass loss rate (MLR) were tested by the cone calorimeter (Fire Testing Technology, UK). All samples (100 × 100 × 3 mm^3) were exposed horizontally to an external heat flux of 35 kW m^{-2}, according to ISO 5660 standard procedures.

Thermogravimetric analysis (TGA) was carried out on a TA Q600 thermogravimetric analyzer (TA). A 2 mg of samples (platinum pan) were heated from room temperature to 600°C at a heating rate of 20°C min^{-1} under air atmosphere with a flowing rate of 50 mL min^{-1}.

Scanning electronic micrograph (SEM) observed on a JEOL JSM-5900LV (JEOL, Japan) was used to investigate the residues of the IFR-PP system, which were obtained after combustion by cone calorimeter tests. SEM graphs of the char residue were recorded after gold coating surface treatment. The tensile strength of the materials was measured using an Instron 4302 material tester according to ASTM D-638, and the Izod notched impact strength was examined using an XJ-40A impact strength tester.

RESULTS AND DISCUSSION

Synthesis and characterization of SPEPA and BSPPO

The synthesis route of BSPPO is shown in Scheme 2. The structure of SPEPA was characterized by FTIR (Fig. 1). The stretching absorptions of —CH_3 and —CH_2— are observed at 2945 and 2903 cm^{-1}, respectively, and the bending absorption of —CH_3 and —CH_2— is at 1466 cm^{-1}. The peaks at 3557 and 1147 cm^{-1} can be assigned to O—H stretching and O—H bending in —OH, respectively. The peak 1014 cm^{-1}

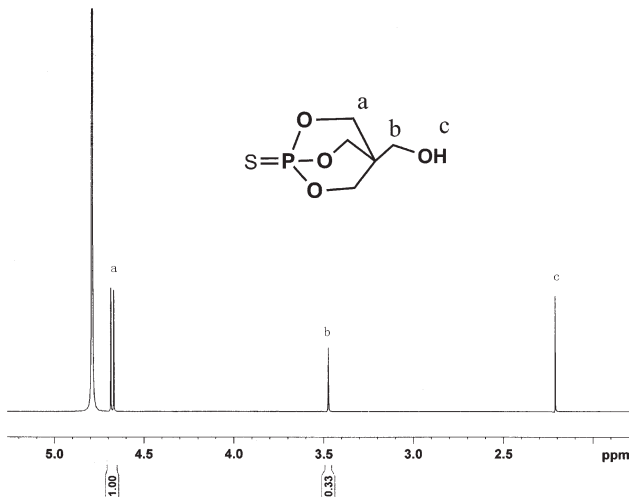

Figure 2 ^{1}H-NMR spectrum of SPEPA.

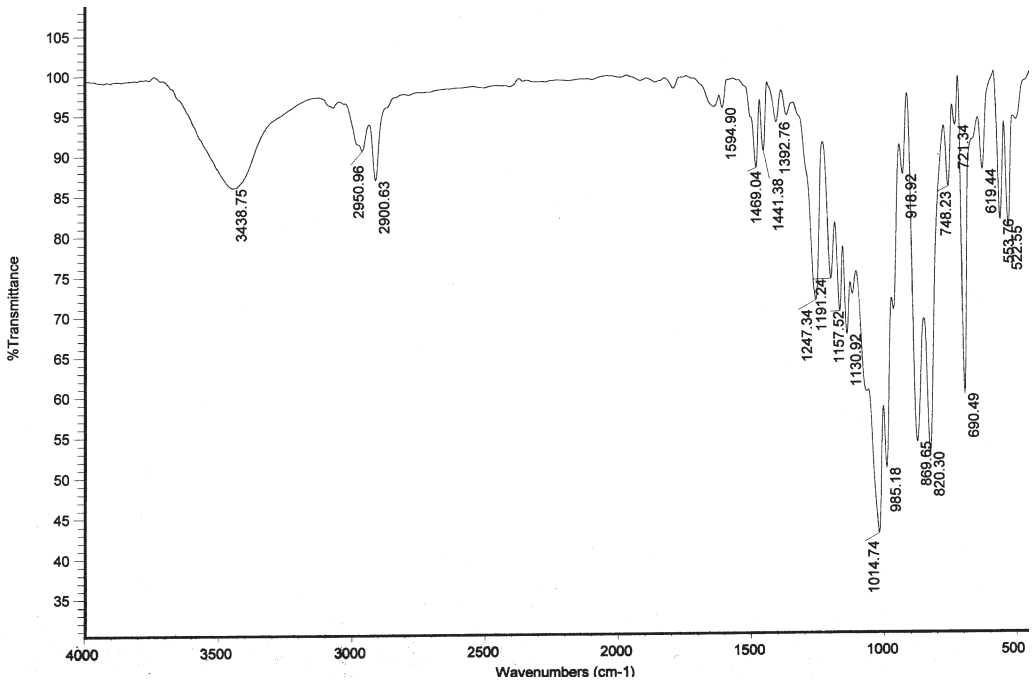

Figure 3 FTIR spectrum of BSPPO.

is associated with P—O—C in the phosphate. The peaks at 867 and 816 cm^{-1} are associated with the stretching mode of caged bicycle $P(OCH_2)_3C$. The peaks at 688 cm^{-1} are associated with the stretching mode of P=S.

The ^{1}H-NMR spectrum of SPEPA is shown in Figure 2. The multiplet between 4.670 and 4.686 ppm (a) corresponds to the —CH_2— protons of the caged bicyclic phosphates. Signal at 3.474 ppm is attributed to the —CH_2— protons (b) adjacent to the caged ring. Signal at 2.212 ppm is attributed to the —OH proton (c).

The previous work[24] confirmed that the crystal structure of SPEPA is three six-membered rings all adopt boat conformations. Molecules form chains along the *C*-axis via intermolecular O—H=O hydrogen bonds. These results prove that the intermediate product has been synthesized successfully.

BSPPO was characterized by FTIR (Fig. 3). The absorption band at about 3058 cm^{-1} corresponds to vibration of benzene ring, and the absorption band at about 748 cm^{-1} corresponds to vibration of single substituted benzene ring. The stretching absorptions of —CH_3 and —CH_2— are observed at 2950, 2900 cm^{-1}, and the bending absorption of —CH_3 and —CH_2— is at 1469 cm^{-1}. Moreover, the peak at 1247 cm^{-1} is associated with the stretching mode of P=O. The peak 1014 cm^{-1} is associated with the stretching mode P—O—C in the phosphate. The peaks at 869 and 820 cm^{-1} are associated with the

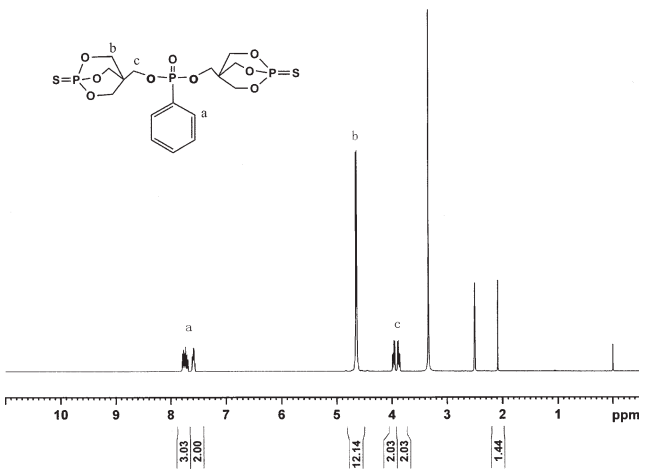

Figure 4 ^{1}H-NMR spectrum of BSPPO.

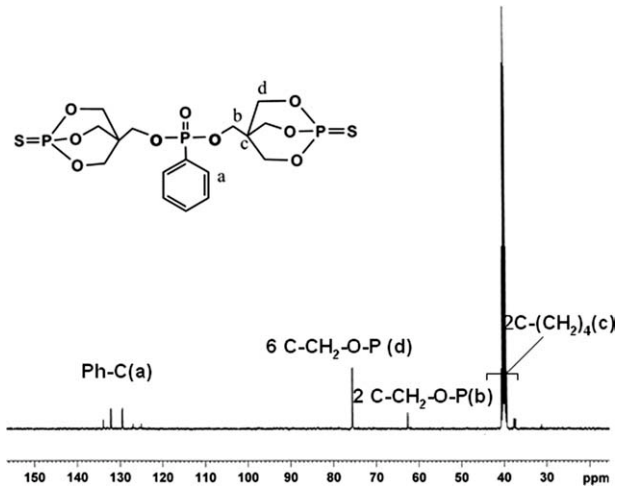

Figure 5 ^{13}C-NMR spectrum of BSPPO.

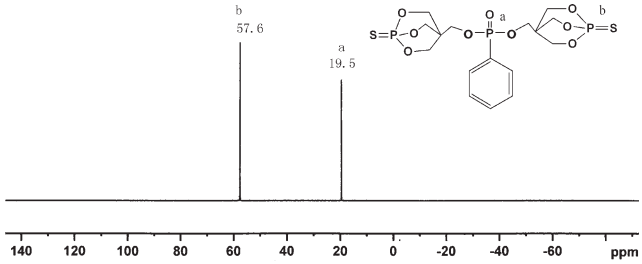

Figure 6 ^{31}P-NMR spectrum of BSPPO.

stretching mode of caged bicycle $P(OCH_2)_3C$. The peaks at 690 cm^{-1} is associated with the stretching mode of P=S.

The ^{1}H-NMR spectrum of BSPPO is shown in Figure 4. The multiplet between 7.57 and 7.79 ppm (a) corresponds to the protons of benzene ring. Signals from 4.63 to 4.65 ppm (b) correspond to the $-CH_2-$ protons of the caged bicyclic phosphates. Signal at 3.474 ppm is attributed to the $-CH_2-$ protons (c) adjacent to the caged ring. The chemical shifts of the absorption peaks and the area ratios of the peak integration are found to be consistent with the expected chemical structure.

The ^{13}C-NMR spectrum of BSPPO is shown in Figure 5. Signals at 40 ppm are attributed to the protons (c) of $C(CH_2)_4$. Signal at 62.64 ppm is attributed to the protons (b) adjacent to the caged ring. The multiplet between 75.5 and 75.7 ppm corresponds to the protons (d) of the caged bicyclic phosphates.[7] The multiplet between 125.0 and 133.9 ppm corresponds to the protons (a) of benzene ring.

The structure of BSPPO is also confirmed by ^{31}P-NMR spectrum illustrated in Figure 6. Two sharp signals are observed. The peak of phosphorus (a) linked with benzene is observed at 19.50 ppm. The peak at 57.6 ppm corresponds to the phosphorus (b) of the caged bicyclic phosphates. From the above analysis, it can be believed that the target product has been synthesized successfully.

Flammability

This novel BSPPO which was synthesized in our work was mixed with APP, MPP, and PP to obtain a new IFR system. To evaluate the flame retardance properties and the synergy of the three components, the LOI and vertical burning test (UL-94) were conducted. The results are given in Table I.

The LOI of the pure PP is only 18.3 with dripping, which indicates that PP is easy to fire. When the three components were added separately (formulations 2, 3, and 4), the LOI of these formulations is not exceed 24, UL-94 ranking is failed, which means the flammability of these systems is not good. The flame retardance is still unsatisfying for the two-component systems of APP/MPP (formulation 5), MPP/BSPPO (formulation 6), and APP/BSPPO (formulation 7). To combine the three components, adding only 2% BSPPO (formulation 5), the flame retardancy is increased greatly. The best ratio of APP, MPP, and BSPPO is 14 : 8 : 8 which LOI is 32, UL-94 is V-0 rating (formulation 11). The results demonstrate that BSPPO is synergy excellently with APP and MPP. Moreover, no dripping was observed during UL-94 test, so the char-forming agent BSPPO shows an excellent antidripping property. The reason may be that with the effective charring agent (BSPPO), the char can be rapidly formed as encountering fire or heat, and change the viscosity of the melting matrix.

The cone calorimetry is one of the most effective bench-scale methods to study the flammability of materials. HRR, especially the PHRR, THR, SPR, and TSP are important parameters for evaluating flame retardancy and flammability of polymeric materials. Figures 7–11 show the combustion plots of pure PP and IFR-PP system (PP + 30% IFR, formulation 11), which were obtained from the cone calorimeter test at a heat flux of 35 kW m^{-2}. Figure 7 indicates that the pure PP burns very rapidly. The HRR increases very fast after ignition, and a sharp HRR peak

TABLE I
Effect of IFR Composition on the Flame Retardance of PP

	Composition of IFR-PP (%)					UL-94	
Formulation	PP	APP	MPP	BSPPO	LOI (%)	Dripping	Ranking
1	100	0	0	0	18.3	Yes	Fail
2	70	30	0	0	22.0	Yes	Fail
3	70	0	30	0	23.6	Yes	Fail
4	70	0	0	30	23.4	Little	Fail
5	70	22.5	7.5	0	24.1	Yes	Fail
6	70	0	22.5	7.5	26.2	Little	V-2
7	70	22.5	0	7.5	25.9	Yes	Fail
8	70	22	6	2	28.5	No	V-0
9	70	18	6	6	30.0	No	V-0
10	70	20	8	2	30.5	No	V-0
11	70	14	8	8	32	No	V-0

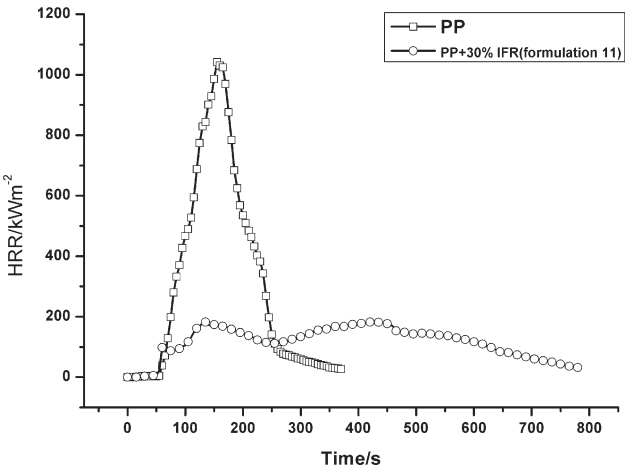

Figure 7 HRR curves of pure PP and IFR-PP system.

(1041.6 kW m^{-2}) appears at 155 s. The IFR-PP burns slowly compared with pure PP. The PHRR decreases from 1041.6 kW m^{-2} to 182.1 kW m^{-2}, which indicates that the flammability of the composite is obviously restrained. It is worth noticing that there are two obvious peaks of the HRR curve of the IFR-PP, which is a typical character of intumescent systems. The first peak is assigned to the ignition and to the flame spread on the surface of the materials and then to protection via the intumescent coating when the HRR values become constant. The material is protected by the intumescent char in this time zone. The second peak means the destruction of the intumescent structure and the formation of a carbonaceous residue.

Figure 8 shows the curves of the THR. The value of THR of IFR-PP is reduced a lot and the THR time is also obviously delayed which compares with that of the pure PP. The release of smoke is another important parameter for the flame-retarded materials. Figures 9 and 10 show the curves of SPR and TSP

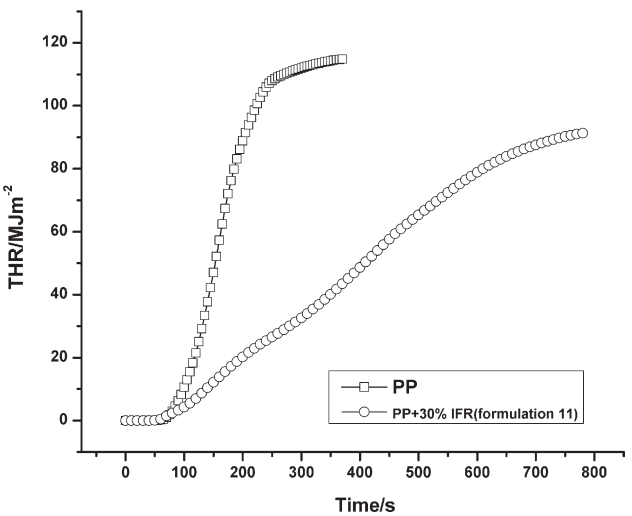

Figure 8 THR curves of pure PP and IFR-PP system.

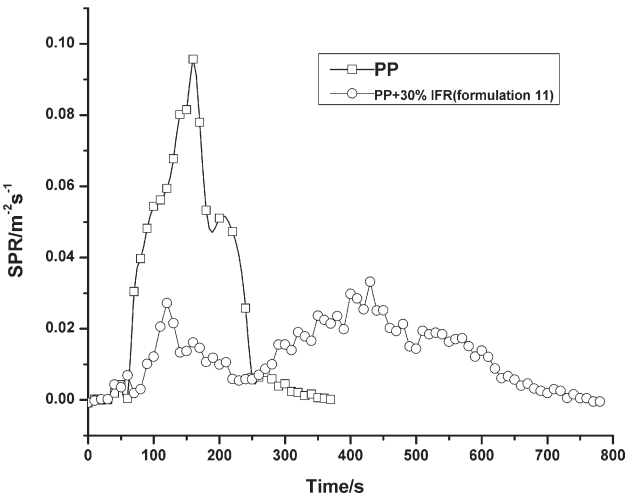

Figure 9 SPR curves of pure PP and IFR-PP system.

via burning time of the pure PP and IFR-PP. During burning, the pure PP and IFR-PP present low smoke emission, and their TSP all are less than 12 m^2. The peak of SPR of PP is 0.095 m^2 s^{-1} at about 160s. With adding IFR, the peak of SPR reduces to 0.03 m^2 s^{-1} at 450 s. It can demonstrate that the smoke emission is retarded and delayed during the whole emission process with APP/BSPPO/MPP system.

The curves of MLR versus combustion time of pure PP and IFR/PP are showed in Figure 11. It can be seen that the IFR could effectively prohibit the decomposition of PP and form an amount of char on the surface. The mass loss behavior of the composite is coincidence with the heat release behavior and the smoke emission behavior. From the data above, we can demonstrate that the heat transfer and flammable vaporing matter transfer between the flame and the polymer decrease greatly, so the flame retardancy of the IFR-PP system is improved a lot.

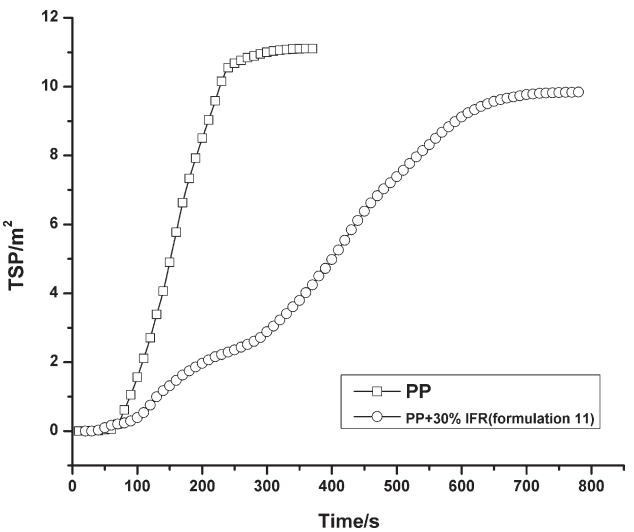

Figure 10 TSP curves of pure PP and IFR-PP system.

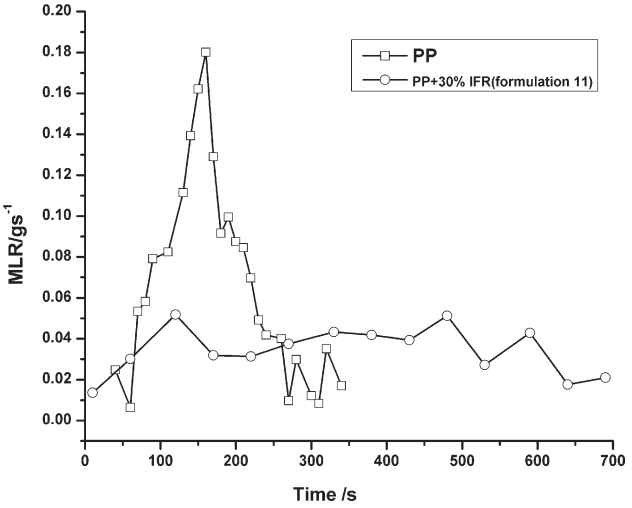

Figure 11 MLR curves of pure PP and IFR-PP system.

The thermal stability of BSPPO and Flame-retardant PP system

TGA is one of the commonly used techniques for rapid evaluation of the thermal stability of different materials, and it can also indicate the decomposition behavior of flame retardants at various temperatures.[25,26] The TGA and DTG curves of the pure PP, BSPPO, and PP + 30% IFR (APP : BSPPO : MPP = 14 : 8 : 8, formulation 11) are shown in Figures 12 and 13. The TGA and DTG curves show that the pure PP decomposes at about 280°C in the air, the maximum decomposition temperature is about 360°C, the char residue is nearly zero. However, the initial decomposition temperature of BSPPO is 320°C with two decomposing steps. The first step occurs at around 330°C which relates to the release of water, to the decomposition and crosslinking reactions, which can protect the matrix from heat and decomposition. The second step occurs at around 400°C

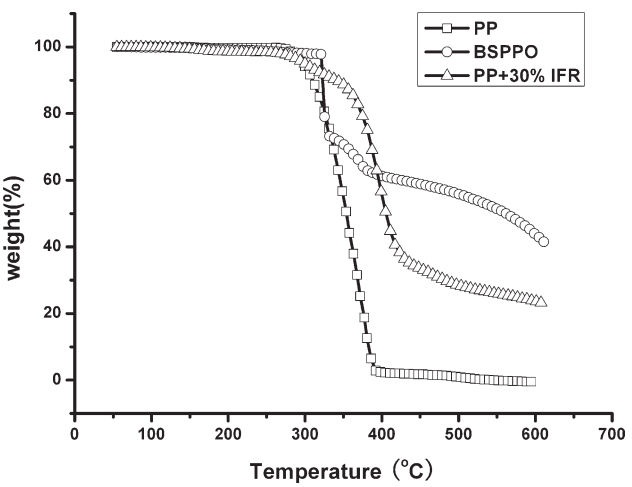

Figure 12 TGA curves of pure PP, BSPPO, and formulation 11 (PP + 30% IFR; air atmosphere and the heating rate is 20°C min^{-1}).

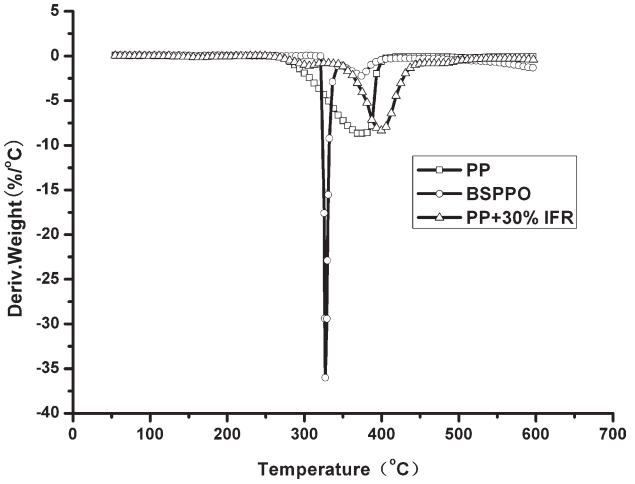

Figure 13 DTG curves of pure PP, BSPPO, and formulation 11 (PP + 30% IFR; air atmosphere and the heating rate is 20°C min^{-1}).

which relates to the further crosslinking, further decomposition, and charring. The BSPPO itself exhibits an excellent char-forming ability, the char residue is as high as 40.6% at 600°C. When the new compound BSPPO is combining with APP and MPP, the char residue is about 22%. The maximum decomposition temperature of the IFR-PP system is about 420°C, which is 60°C higher than pure PP. This further proves the results of LOI, UL-94, and cone calorimeter, so BSPPO is an excellent carbon agent for PP combined with APP and MPP.

The flame retardance mechanism

FTIR characterization of the residue

The char residue plays an important role in the flame retardance of PP. To better understand the flame retardance mechanism and the synergistic role of the IFR, the properties of combustion residue were investigated by FTIR and SEM. Figure 14 shows the FTIR spectrum of the residue after IFR-PP system was heating 10 min under 600°C in muffle furnace. The absorption band at about 3422 cm^{-1} is assigned to the stretching mode of —OH from the P—OH group, and the bands at 3120 and 1401 cm^{-1} correspond to the stretching mode of —NH in NH_4^+. The absorption at 2361 cm^{-1} is assigned to the stretching mode of P—H. Moreover, the absorption band at 1643 cm^{-1} is assigned to the stretching mode of aromatic compound, and the peaks at 1005 and 925 cm^{-1} are attributed to the symmetric and asymmetric vibration of P—O in P—O—P group.[27] Therefore, the FTIR spectrum confirms the existence of P—OH, P—H, P—O—P, and NH_4^+ groups in charred layers, which means that NH_3 and polyphosphoric acid are produced at high temperature. Polyphosphoric acid is contributed to the carbonization of BSPPO and the degradation and

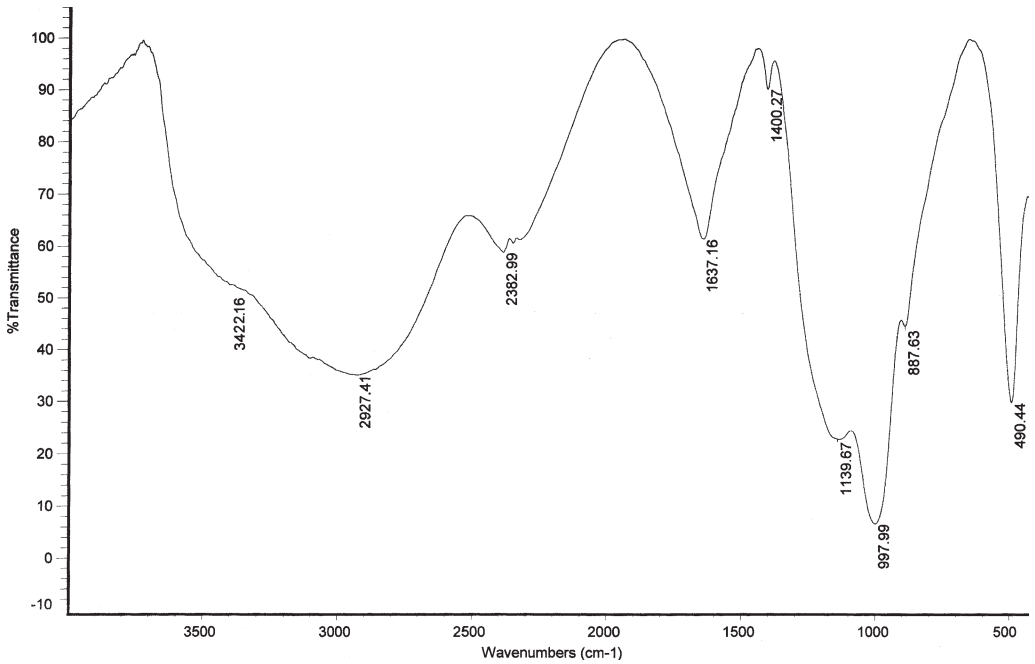

Figure 14 FTIR spectrum of the residue after the IFR-PP system was heating 10 min under 600°C in the muffle furnace.

charring of PP, which reverts to phosphoric acid through this process. NH_3 produced by APP or MPP dilutes the concentration of the oxygen near the surface of material and foams the carbon layer during fire. Furthermore, MPP because of its three amidocyanogen can react with phosphoric acid to form a crosslink structure, which acts as a barrier to limit the diffusion of both the volatile thermal oxidative products to the gas phase and oxygen from the gas phase to the matrix.

The morphology of the char residue

Figure 15 shows the SEM images of the char residues of IFR-PP after cone calorimeter test. It can be seen that the surface of char is smooth and tight, indicating a dense char structure. During combustion a high-quality char can effectively form a protected layer to prevent the melted PP from dripping, enhance the dripping resistance, and protect the matrix under the char layer which is coincident with the literature.[8]

Mechanical performance of PP/IFR system and effect of water solubility of IFR on the performance of PP/IFR system

To evaluate the effect of the water solubility of APP/BSPPO/MPP system on the performance of PP/IFR, the samples have been poached in water at 70°C for 7 days. Table II lists the mechanical and flame properties of PP/IFR systems and PP/IFR systems poached in water. The tensile strength, elongation at break, and Izod notched impact strength of

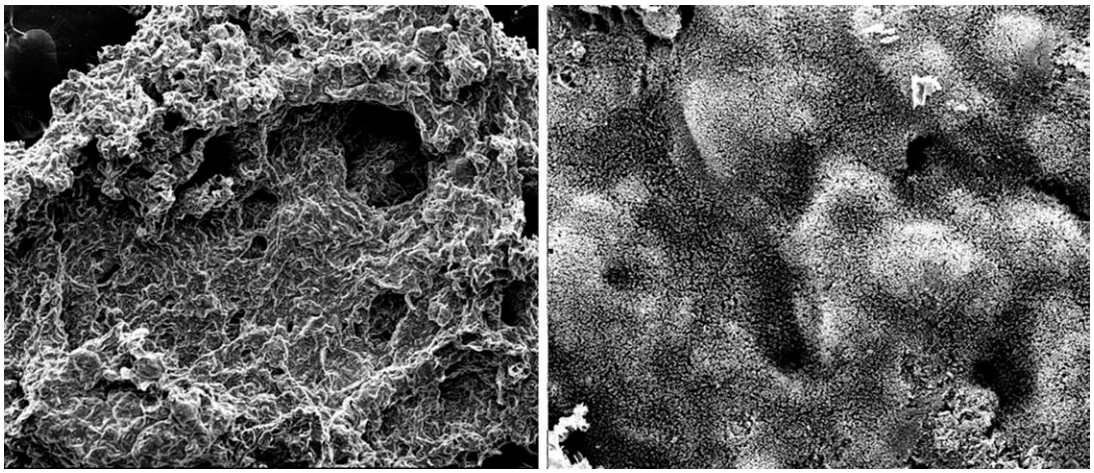

Figure 15 SEM images of the char residues after cone calorimeter test.

TABLE II
Mechanical and Flame Properties of PP/IFR and PP/IFR Poached in Water

	Mechanical properties				UL-94		
	Tensile strength (MPa)	Elongation at break (%)	Izod notched impact strength (kJ m^{-2})	LOI (%)	Dripping	Ranking	Weight variation after poached (%)
Pure PP	30.5	686	8.6	18.3	Yes	Fail	N/A
PP/IFR (formulation 11)	24.18	81	5.96	32.0	No	V-0	N/A
PP/IFR[a] (APP : MPP : PER = 3 : 1 : 1)	23.5	78	5.32	27.9	A little	V-1	N/A
PP/IFR[a] (poached; APP : MPP : PER = 3 : 1 : 1)	23.4	63	5.34	24.8	Yes	Fail	−2.8
PP/IFR (poached; formulation 11)	24.20	70	5.97	28.6	No	V-0	−0.3

[a] Flame retardant loading level: 30%.

PP/IFR are decreased much comparing to pure PP. When the samples were poached in water, there is a little effect on the mechanical properties. The weight of samples is decreased 0.3% for BSPPO IFR system (formulation 11), whereas the weight of samples is decreased 2.8% for PER IFR system. Although the LOI of BSPPO IFR system is decreased a lot as same as PER IFR system, the UL-94 rating of BSPPO IFR system is not deteriorated. The results demonstrate that the antiwater-solubility of the BSPPO IFR system is improved comparing to the PER IFR system, and the flame retardance is also improved.

CONCLUSIONS

A novel charring agent of BSPPO was successfully synthesized. The IFR using BSPPO as carbonization agent shows excellent flame retardancy and antidripping properties for PP. The synergistic effect among APP (acid source), MPP (gas source), and the new synthesized charring agent, BSPPO, is pivotal to fully exert the flame retardance of the IFR system. The optimum flame retardant formulation is APP : MPP : BSPPO = 14 : 8 : 8 (LOI is 32, UL-94 V-0 rating, PHRR is 182.1 kW m^{-2}, and SPR is 0.03 m^2 s^{-1}). The cone calorimeter tests agree very well with the TG analysis, which confirm the excellent char-forming ability of BSPPO. The char properties were also characterized by FTIR spectroscopy and SEM micrograph which prove the char quantity and quality formed during combustion are crucial to the flame retardance and antidripping ability of the IFR-PP system. The antiwater-solubility of IFR system with BSPPO is improved.

Authors wish to thank the FTIR, nuclear magnetic resonance, and SEM analyses assistance provided by Analysis and Testing Center of Sichuan University and the cone calorimeter test assistance provided by Chinese State Key Laboratory of Polymer Materials Engineering.

References

1. Sen, A. K.; Mukherjee, B.; Bhattacharya, A. S.; Sanghi, L. K.; De, P. P.; Bhowmick, A. K. J Appl Polym Sci 1991, 43, 1673.
2. Pfaendner, R. Polym Degrad Stab 2006, 91, 2249.
3. Bourbigot, S.; Duquesne, S. J Mater Chem 2007, 17, 2283.
4. Wu, J.; Hu, Y.; Lei, S. Polym Plast Technol 2008, l47, 1205.
5. Haurie, L.; Fernandez, A. I.; Velasco, J. I.; Chimenos, J. M.; Cuesta, J. M. L.; Espiell, F. Polym Degrad Stab 2006, 91, 989.
6. La Rosa, A. D.; Motta, O.; Recca, A. J Polym Eng 2002, 22, 341.
7. Fontaine, G.; Bourbigot, S.; Duquesne, S. Polym Degrad Stab 2008, 93, 68.
8. Peng, H. Q.; Zhou, Q.; Wang, D. Y.; Chen, L.; Wang, Y. Z. J Ind Eng Chem 2008, 14, 589.
9. Liu, Y.; Deng, C. L.; Zhao, J.; Wang, J. S.; Chen, L.; Wang, Y. Z. Polym Degrad Stab 2010; doi:10.1016/j.polymdegradstab.2010.02.033.
10. Le Bras, M.; Bugajny, M.; Lefebvre, J. M.; Bourbigot, S. Polym Int 2000, 49, 1115.
11. Ma, Z. L.; Zhao, M.; Hu, H. F.; Ding, H. T.; Zhang, J. J Appl Polym Sci 2002, 83, 3128.
12. Chen, Y.; Liu, Y.; Wang, Q.; Yin, H.; Aelmans, N.; Kierkels, R. Polym Degrad Stab 2003, 81, 215.
13. Chen, X.; Ding, Y.; Tang, T. Polym Int 2005, 54, 904.
14. Li, Q.; Zhong, H. F.; Wei, P.; Jiang, P. K. J Appl Polym Sci 2005, 98, 2487.
15. Xie, F.; Wang, Y. Z.; Yang, B.; Liu, Y. Macromol Mater Eng 2006, 291, 247.
16. Li, Q.; Jiang, P.; Su, Z.; Wei, P.; Wang, G.; Tang, X. J Appl Polym Sci 2005, 96, 854.
17. Le Bras, M.; Bourbigot, S.; Delporte, C.; Siat, C.; Le Tallec, Y. Fire Mater 1996, 20, 191.
18. Lewin, M.; Endo, M. Polym Adv Technol 2003, 14, 3.
19. Youssef, B.; Mortaigne, B.; Soulard, M.; Saiter, J. M. J Therm Anal Calorim 2007, 90, 489.
20. Giraud, S.; Bourbigot, S.; Rochery, M.; Vroman, I.; Tighzert, L.; Delobel, R.; Poutch, F. Polym Degrad Stab 2005, 88, 106.
21. Liu, Y.; Wang, Q. Polym Degrad Stab 2006, 91, 2513.
22. Wang, C. S.; Lin, C. H.; Chen, C. Y. J Polym Sci Part A: Polym Chem 1998, 36, 964.
23. Ratz, R.; Sweeting, O. J. J Org Chem 1965, 30, 438.
24. Yang, Q.; Zhang, Y. Q.; Huang, J. Q.; Men, J.; Gao, G. W. Acta Crystallogr Sect E Struct Rep Online 2008, 65, o141.
25. Cullis, C. F.; Hirschler, M. M. Polymer 1983, 24, 834.
26. Hirschler, M. M. Eur Polym Mater 1983, 19, 121.
27. Michel, B.; Bourbigot, S.; Michel, L.; Bras, R. D. Polym Int 1999, 48, 264.